Journal of Science: Advanced Materials and Devices 1 (2016) 98–102

Contents lists available at ScienceDirect

Journal of Science: Advanced Materials and Devices

journal homepage: www.elsevier.com/locate/jsamd

Original article

Detection of magnetic nanoparticles using simple AMR sensors in Wheatstone bridge

L.K. Quynh, B.D. Tu, D.X. Dang, D.Q. Viet, L.T. Hien, D.T. Huong Giang, N.H. Duc*

VNU Key Laboratory for Micro-nano Technology and Faculty of Physics Engineering and Nanotechnology, VNU University of Engineering and Technology, Vietnam National University, Hanoi, 144 Xuan Thuy Road, Cau Giay, Hanoi, Viet Nam

A R T I C L E I N F O

Article history:
Received 11 April 2016
Accepted 16 April 2016
Available online 22 April 2016

Keywords:
Anisotropic magnetoresistance
Wheastone bridge
Magnetic sensor
Magnetic nanoparticle detection

A B S T R A C T

Wheatstone bridges incorporating a serially connected ensemble of simple AMR elements of $Ni_{80}Fe_{20}$ film were produced, targeting an application of a pinned magnetic field along the sensing magnetoresistor length. For the optimal dimension, the magnetoresistive element with length $l = 4$ mm, width $w = 150$ μm and thickness $t = 5$ nm still shows a rather modest AMR ratio (of about 0.85% only). However, the resulting bridge exhibits a sensitivity as large as 2.15 mV/Oe. This is according to a standard sensitivity of 1.80 mV/V/Oe and a detection limit better than 10^{-6} emu, which is almost doubled with respect to that in the typical commercial AMR devices and is comparable with Permalloy based PHE sensor. This is suitable to detect the superparamagnetic fluid of 50 nm-Fe_3O_4-chitosan.

1. Introduction

Spintronic sensors have been becoming increasingly important not only in industrial domains, but also in biomedical applications. For latter interests, the magnetic microbeads or nanoparticles are labeled with biomolecules and are employed in detecting target by binding the probe biomolecules immobilized on the magnetic sensing surface. Accordingly, magnetic sensing micro-bioassays have been developed on the basis of anisotropic magnetoresistive (AMR), giant magnetoresistive (GMR), magnetic tunnel junction (MTJ) and/or planar Hall effect (PHE) sensors [1,2]. In such applications, the magnetic field sensitivity of about 10 μV/Oe and the detection limit of 2×10^{-10} emu is required [2,3]. In addition, the stability of the sensor output must be ensured over a large range of temperatures and, in general, the signal to noise (*S/N*) ratio must be suppressed. These demands are usually improved thanks to integrating the sensors in Wheatstone bridge configuration, which can provide a null-voltage output in the absence of an external stimulation field, while ensuring the same full output voltage of a single device [4–6]. Practically, a classic Wheatstone bridge was designed based on typical 0°–90° AMR magnetoresistors [4]. The replacement of AMR by MTJ sensors resulted in devices with enhanced magnetic field sensitivity of 32 mV/V/Oe [5], which strongly overcomes the sensitivity of 1 mV/V/Oe in the typical commercial products integrating AMR devices in bridge configuration. Recently, the possibility to use the Wheatstone bridge of exchange-biased GMR spin valve sensors for the detection of 10-nm iron oxide nanoparticles with the concentration of 10 ng/ml was reported [6]. This makes the spintronic sensors rather suitable for use as a biomedical detector.

In this paper, we investigated the possibility of detecting superparamagnetic 50-nm iron oxide nanoparticle utilizing simple AMR sensors in Wheatstone bridge. Here, the low field magnetic sensitivity of AMR bridge device is enhanced by optimizing the dimension of single magnetoresitors correspondingly to their shape magnetic anisotropy.

2. Experimental

The 4 mm-length AMR elements of $Fe_{80}Ni_{20}$ Permalloy with different wide ($w = 150$, 300 and 450 μm) and thickness ($t = 5$, 10 and 15 nm) and respective AMR Wheatstone bridges (see *e.g.* in Fig. 1) were fabricated by using magnetron sputtering technology (*Model ATC* 2000) and the UV Lithography technology (*Model MJB*4). The top Ta layer thickness is of 5 nm. During sputtering process, the magnetic uniaxial anisotropy of single AMR elements was established thanks to a permanent magnet which generated a pined magnetic field of $H_{pin} = 900$ Oe along the sensing R_1 and R_3 magnetoresistor length (Fig. 1c). The pinning degree on this resistor

* Corresponding author.
E-mail address: ducnh@vnu.edu.vn (N.H. Duc).
Peer review under responsibility of Vietnam National University, Hanoi.

http://dx.doi.org/10.1016/j.jsamd.2016.04.006
2468-2179/

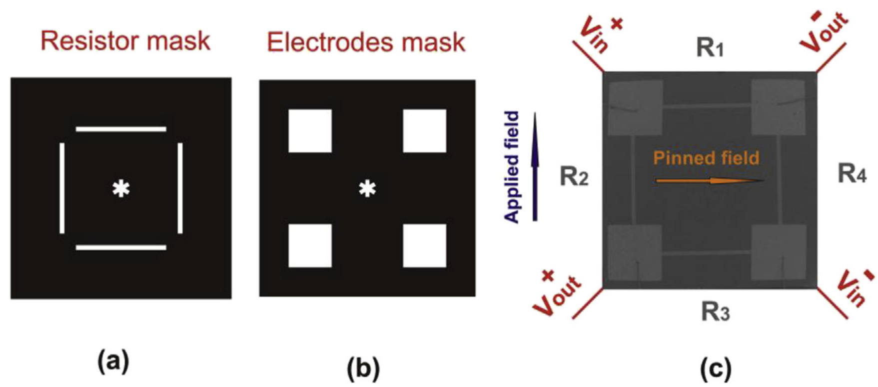

Fig. 1. Fabrication process of AMR elements and complete AMR Wheatstone bridges: (a) resistor mask, (b) electrodes mask, (c) image of fabricated sensor and respective Wheatstone bridge.

pair is different with respect to that on (R_2, R_4) ones due to the shape magnetic anisotropy. Thus, in applied fields, the resistance in (R_1, R_3) and (R_2, R_4) pairs is varied in different ways.

For magnetoresistance measurement, the *dc* precision current source was supplied by using *Keithley* 6220 and the output voltage (V_{out}) was recorded by *Keithley* 2000 multimeter. The V_{out} voltage of the Wheatstone bridge was detected by DSP lock-in amplifier (*Model 7265 of Signal Recovery*) combining with an oscilloscope (*Tektronic DP* 4032).

The output voltage is created due to the different resistance changes. In this case, the change in output voltage (ΔV_{out}) of the Wheatstone bridge is given as

$$\Delta V_{out} = V_{in}(R_1 - R_2)/(R_1 + R_2)$$

where V_{in} is the input voltage and $R_1 = R_3$, $R_2 = R_4$.

In the measuring setup, a *dc* current was applied to the Wheatstone bridge for output voltage measurements. For small resistance change, this constant-current mode is preferred to have more linear response and higher sensitivity (than using constant-voltage mode) [7].

3. Results and discussions

3.1. AMR of magnetoresistive elements

The field dependence of AMR ratio was investigated for a single 4 mm-length AMR element of FeNi with different width ($w = 150$, 300 and 450 μm) and thickness ($t = 15$ nm). The data were recorded with the supplied current of 1 mA and in external magnetic fields applied perpendicular to the pinned magnetic field direction. Here, the ARM ratio is given as

$$AMR(\%) = \frac{\Delta R}{R_{min}} = \frac{R(H) - R_{min}}{R_{min}} = \frac{V(H) - V_{min}}{V_{min}}$$

Presented in Fig. 2 is AMR data measured for the sensing magnetoresistor, which is pinned along the sensor length (i.e. R_1 and/or R_3). It can be seen from this figure that for samples of the same length and thickness, the wider resistor bar, the lower AMR effect is obtained. Indeed, only the highest AMR of 0.34% was found in the sample with $w = 150$ μm. The AMR decreases down to 0.15% for $w = 450$ μm. Similarly, the slope of AMR curves also decreases with increasing *w*. This finding may reflect a well established uniaxial magnetic anisotropy (along the length and/or pinned direction) in resistor elements having a small demagnetizing factor, *i.e.* small *w* demension. A much worse AMR is found for the magnetoresitors,

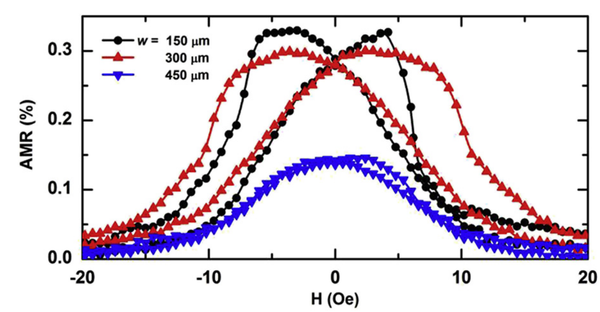

Fig. 2. Magnetic field dependence of AMR ratio measured in external fields applied along the pinned direction for single 4 mm-length AMR elements of FeNi with different width ($w = 150$, 300 and 450 μm) and thickness ($t = 15$ nm).

where the pinned field is perpendicular to the sensor length (*i.e.* R_2 and/or R_4).

The AMR is enhanced in thinner films. For the optimal dimension, the magnetoresistive element with length $l = 4$ mm, width $w = 150$ μm and thickness $t = 5$ nm exhibits a modest AMR ratio of about 0.85%.

3.2. Wheatstone bridge output voltage

As already reported above, in all single magnetoresistive elements under investigation, the AMR signal is not so stable (see *e.g.* Fig. 1). Principally, this is considered as a partial contribution from the thermal noise. It can usually be solved by integrating magnetoresistors in Wheatstone bridge configuration as designed and fabricated in Fig. 1. In this case, the output signals recorded at a supplied current of 1 mA are illustrated in Fig. 3a for AMR Wheatstone bridge integrating single 4 mm-length AMR elements of FeNi with different width ($w = 150$, 300 and 450 μm) and thickness ($t = 15$ nm). Their respective magnetic field derivative d*V*/d*H* is presented in Fig. 3b. Clearly, higher stable data are observed. The output voltage of 1.63 mV and maximal sensitivity of 0.24 mV/Oe are found for the Wheatstone bridge with 450 μm width AMR sensors. They strongly increase up to 3.28 mV and 1.05 mV/Oe, respectively, in the 150 μm width sensors.

The NiFe-layer thickness dependence of the output voltage was investigated in three of constant 4 × 0.45 mm area sensors with $t = 5$, 10 and 15 nm. The results are shown in Fig. 4. It can be seen that the thinner NiFe layer, the higher output signal and sensitivity are obtained. Indeed, for the device with $t = 5$ nm, the highest output voltage change $\Delta V = 3.98$ mV and sensitivity $S_H = (dV/$

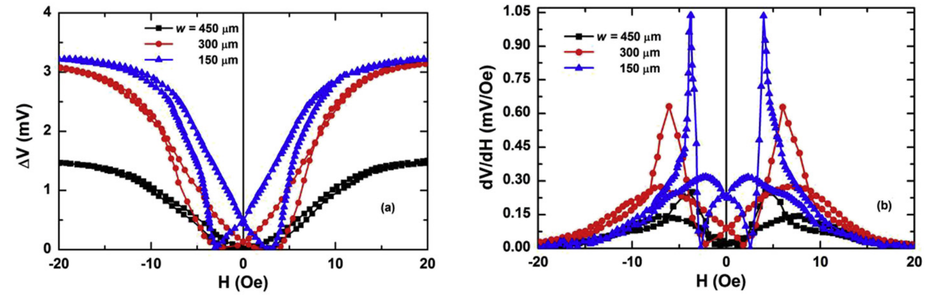

Fig. 3. Magnetic field dependence of output voltage (a) and relative derivative (b) of AMR Wheatstone bridge integrating single 4 mm-length AMR elements of FeNi with different width (w = 150, 300 and 450 μm) and thickness (t = 15 nm).

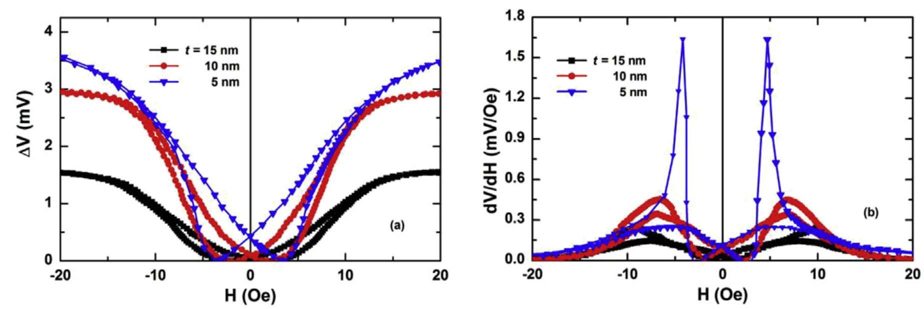

Fig. 4. Magnetic field dependence of output voltage (a) and relative derivative (b) of AMR Wheatstone bridge integrating single 4 × 0.45 mm^2-area AMR elements of FeNi with different thickness t = 5, 10 and 15 nm.

dH) = 1.65 mV/Oe. Data are collected and listed in Table 1. The variation of investigated Wheatstone bridge output parameters usually relate to magnetoresistive intrinsic properties and mechanism. Here, however, the shape magnetic anisotropy contribution, *i.e.* the $(w \times t)/l$ ratio and respective demagnetizing factor seems to exhibit systematically.

As regards the shape magnetic anisotropy, the optimal AMR element dimension of 4 × 150 × 5 (mm × μm × nm) is approached. For this case, the Wheatstone bridge output voltage and respective derivative data are presented in Fig. 5. It is interesting that this sensor configuration exhibits a smallest coercivity H_c = 2.6 Oe. At a *dc* current of 1 mA, the ouput voltage and respective voltage sensitivity reach the highest values of ΔV = 7.6 mV and S_H = 2.15 mV/Oe. As a consequence, a standard sensitivity of 1.80 mV/V/Oe was calibrated for the input voltage V_{in} = 1 V, which is almost doubled with respect to that in the typical commercial AMR devices. This observed voltage sensitivity is increased near 10 times in comparison with the that of the largest AMR element dimension of 4 × 450 × 15 (mm × μm × nm). Note that, the voltage sensitivity can be further enhanced by increasing the supplied current (see also Fig. 5). At a current of 4 mA, values of ΔV = 30.8 mV and S_H = 9.85 mV/Oe, i.e. corresponding to the standard sensitivity of 2.05 mV/V/Oe.

Table 1
The output voltage change ΔV and the magnetic sensitivity S_H (=dV/dH) measured in the 1 mA current constant mode for different single AMR element dimension ($l \times w \times t$).

No	$l \times w \times t$ (mm × μm × nm)	ΔV (mV)	S_H (mV/Oe)
1	4 × 150 × 15	3.28	1.05
2	4 × 300 × 15	3.20	0.70
3	4 × 450 × 15	1.63	0.25
4	4 × 450 × 10	3.02	0.45
5	4 × 450 × 5	3.98	1.65
6	4 × 150 × 5	7.6	2.15

3.3. *Magnetic nanoparticle detection*

Magnetic nanoparticles detection was tested by using the Wheatstone bridge device with optimal magnetoresistor dimension of 4 × 150 × 5 (mm × μm × nm). Experimental setup is illustrated in Fig. 6. The investigation is performed with the superparamagnetic fluid of Fe_3O_4-chitosan with diameter of 50 nm and concentration of 10 mg/ml. During the measurement, the magnetic nanoparticles were dropped directly on the sensing magnetoresistor surface. Iron oxide nanoparticles were magnetized out-of-plane in the magnetic field of about 100 Oe created by a permanent magnet placed closed to the sensor (Fig. 6a) while the sensors are sensitive to the in-plane component of the stray field emanated from those superparamagnetic nanoparticles. The Helmholtz coils (Fig. 6b) were supplied a constant *dc* current to provide an in-plane magnetic field around 3.5 Oe, which can place the AMR sensor bridge at its most sensitive operating point. Note that, this magnetic field is perpendicular to the pinned magnetic field (Fig. 6c). From the magnetization data [8], the magnetic nanoparticles exhibit a magnetization as large as 2 emu/g only.

The output voltage signals versus time trace for nanoparticle detection are plotted in Fig. 7. In the absence of magnetic nanoparticles, the signal exhibit a background noise resolution of about 0.01 mV. The presence of an amount of 0.1 μl of magnetic nanoparticles solution causes an output voltage change as large as 0.025 mV, which corresponds to a detection possibility of 2×10^{-6} emu. This detection limit is almost 2 order of magnitude lower than that of magnetic sensors based on the magnetoelectric effect [8,9], but is comparable that recently reported to the Permalloy based PHE sensor [10]. In addition, it is consistent with the magnitude expected for the geo-magnetic field. In the presence of 0.2 μl of magnetic nanoparticles solution, the output voltage change increased by more than twice (*i.e.* upto 0.055 mV). This result makes this simple AMR sensor rather promising for detection of magnetic beads in biomedical applications.

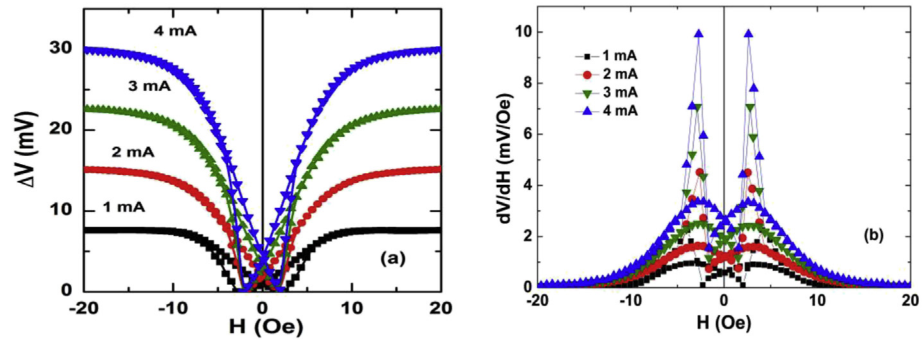

Fig. 5. Magnetic field dependence of output voltage (a) and relative derivative (b) of AMR Wheatstone bridge integrating single 4 × 150 × 5 (mm × μm × nm) AMR elements of FeNi at different *dc* currents.

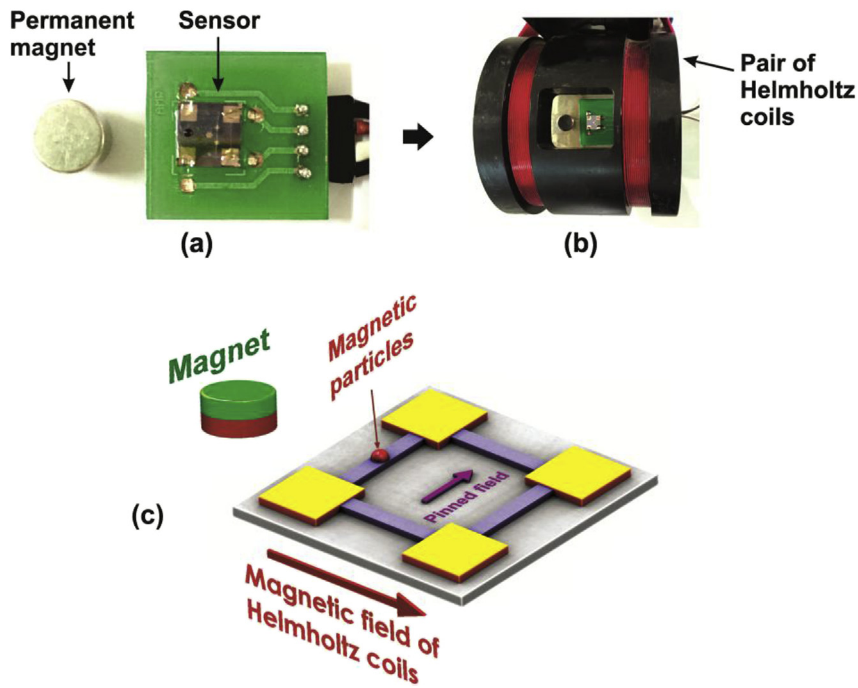

Fig. 6. The experimental setup for detection of magnetic particles: images of AMR Wheatstone bridge device and permanent magnet (a) in Helmholtz coils (b) and the configuration of magnetic field components (c).

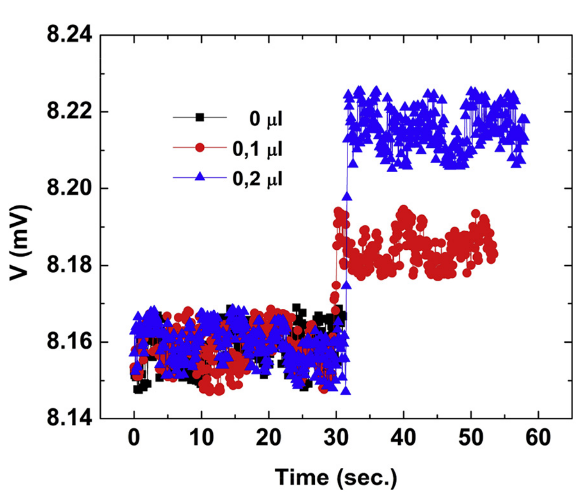

Fig. 7. Output voltage versus time trace tested by using the Wheatstone bridge device with AMR sensor dimension of 4 × 150 × 5 (mm × μm × nm).

4. Conclusions

Simple chips with 4 Permalloy AMR sensors were designed and fabricated. Wheatstone bridges incorporating a serially connected ensemble of AMR elements were produced, targeting an application of a pinned magnetic field along the sensing magnetoresistor length. The optimization of the shape magnetic anisotropy enhanced the device sensitivity up to 2.15 mV/Oe. The detection limit better than 10^{-6} emu is reached. This is almost doubled with respect to that in the typical commercial AMR devices and is comparable with Permalloy based PHE sensor. This is suitable to detect the magnetic nanoparticles. The results suggest that if one can increase the S/N ratio, this type of structure is feasible for building low cost micrometer sized AMR chips to be used for high-resolution biosensing applications.

Acknowledgments

This work was supported by the National Research Program on Space Technology of Vietnam under the granted Research Project

No. VT/CN-03/13-15 and Vietnam National University, Hanoi under the granted Research Project No. QGTĐ13.24.

References

[1] P.P. Freitas, H.A. Ferreira, D.L. Graham, L.A. Clarke, M.D. Amaral, V. Martins, L. Fonseca, J.S. Cabral, in: M. Johnson (Ed.), Magnetoelectronics, Elsevier, Amsterdam, 2004.

[2] H. Kim, V. Reddy, K. Woo Kim, I. Jeong, X.H. Hu, C.G. Kim, Single magnetic bead detection in a microfluidic chip using planar hall effect sensor, J. Magn. 19 (2014) 10.

[3] B.D. Tu, L.V. Cuong, T.Q. Hung, D.T. Huong Giang, T.M. Danh, N.H. Duc, C.G. Kim, Optimization of spin-valve structure NiFe/Cu/NiFe/IrMn for planar hall effect based biochips, IEEE Trans. Magn. 45 (2009) 2374.

[4] M.J. Haji-Sheikh, Y. Yoo, An accurate model of a highly ordered 81/19 Permalloy AMR Wheatstone bridge sensor against a 48 pole pair ring-magnet, Int. J. Intell. Syst. Technol. Appl. 3 (2007) 95.

[5] R. Ferreira, E. Paz, P.P. Freitas, J. Ribeiro, J. Germano, L. Sousa, 2-axis magnetometers based on full Wheatstone bridges incorporating magnetic tunnel junctions connected in series, IEEE Trans. Magn. 48 (2012) 4017.

[6] L. Li, K.Y. Mak, C.W. Leung, S.M. Ng, Z.Q. Lei, P.W.T. Pong, Detection of 10-nm superparamagnetic iron oxide nanoparticles using exchange-biased GMR sensors in Wheatstone bridge, IEEE Trans. Magn. 49 (2013) 4056.

[7] N. Mathivanan, PC-Based Instrumentation: Concepts and Practice, Prentice-Hall of India Pvt. Limited, 2007.

[8] D.T. Huong Giang, D.X. Dang, N.X. Toan, N.V. Tuan and N.H. Duc, Distance magnetic nanoparticle detection using a magnetoelectric sensor for clinical interventions, submitted to Sensor and Actuator B.

[9] S. Dong, J. Zhai, N. Wang, F. Bai, J.F. Li, D. Viehland, T.A. Lograsso, Fe-Ga/$PbMg_{1/3}Nb_{2/3}O_3$–$PbTiO_3$ magnetoelectric laminate composites, Appl. Phys. Lett. 87 (2005) 222504.

[10] M. Volmer, M. Avram, Using permalloy based planar Hall effect sensors to capture and detect superparamagnetic beads for lab on a chip applications, J. Magn. Magn. Mater. 381 (2015) 481.